# A Single-Phase Current-Source Converter Combined with a Hybrid Converter for Interfacing an Electric Vehicle and a Renewable Energy Source

Catia F. Oliveira, Ana M. C. Rodrigues, Delfim Pedrosa,
Joao L. Afonso, Vitor Monteiro

ALGORITMI Research Centre, University of Minho, Guimarães, Portugal
c.oliveira@dei.uminho.pt

**Abstract.** This paper presents a single-phase current-source converter (CSC) combined with a hybrid converter on the dc-link, allowing to interface an electric vehicle (EV) and a renewable energy source (RES). Therefore, the interface with the power grid is only performed through the CSC, which also permits the operation as shunt active power filter, allowing to compensate power quality problems related with current. The whole system is composed by two main power stages, namely, the CSC that is responsible for compensating the current harmonics and low power factor, as well as operating as a grid-tied inverter or as an active rectifier, and the hybrid converter that is responsible for interfacing the dc-link of the CSC with the converters for the EV and the RES interfaces. As demonstrated along the paper, the CSC, combined with the hybrid converter on the dc-link, allows the operation as shunt active power filter, as well as the operation in bidirectional mode, specifically for the EV operation, and also for injecting power from the RES. In the paper, the power electronics structure is described and the principle of operation is introduced, supported by the description of the control algorithms. The validation results show the proper operation of the CSC, combined with the hybrid converter on the dc-link, for the main conditions of operation, namely exchanging power with the power grid in bidirectional mode and operating as a shunt active power filter.

**Keywords:** Current-Source Converter, Electric Vehicle, Hybrid Converter, Renewable Energy Source, Power Quality.

## 1 Introduction

Currently, the increasing greenhouse emissions caused by conventional vehicles and the demand for electricity is a huge concern. In order to contribute for a more sustainable mobility, the electric vehicle (EV) has been seen as an efficient solution. Moreover, the EV can also be managed for storing and delivering power during the intermittence of the renewable energy sources (RES) [1]. Thus, the EV can be used as an energy storage system (ESS), permitting to store the energy in periods where the RES production is excessive and in periods of intermittence, deliver the energy back to the installation contributing to balance the power management and consumption [2]. The

integration of the EV and RES in the power grid can introduce power quality problems, such as current harmonics and low power factor, due to the require power converters to interface the power grid [3-5]. The interface of the EV and RES with the power grid is performed by an ac-dc converter and by a dc-dc converter. The dc-dc converter ensures a controllable voltage and current of the dc interfaces, whereas the ac-dc converter is responsible to guarantee sinusoidal currents with low harmonic distortion and unitary power factor [6]. Depending on the dc-link, the ac-dc converter can be voltage-source converter (VSC) or current-source converter (CSC). The VSC has as main drawback the high capacitor used in the dc-link. Usually, the type of capacitors that composes the dc-link are electrolytic that have a lower lifetime comparing with the inductors used in dc-link of the CSC. Besides, the CSC presents as main advantages a good current control and a short-circuit protection capability. Due to these advantages, the CSC can be applied in some power electronic applications, such as in the interface of RES, active power filters and motor drives [7]. Nevertheless, in order to maintain an acceptable level of current ripple in dc-link, it is required a large dc-link inductor for CSC [8][9]. In order to reduce the inductance value and consequently the size and costs of this inductor, a hybrid converter is proposed in [10] for a four-wire current-source shunt active power filter (SAPF), whose structure can also be applied for a single-phase CSC controlled as SAPF, as shown in [11]. Taking into account the perspective of controlling the EV in bidirectional mode for a smart grid perspective, the interface of a conventional CSC with EV is more difficult due to the fact that the CSC is unidirectional. However, the CSC combined with a hybrid converter on the dc-link, can also be used for EV applications, as it is presented in [12]. Additionally, it can also be applied as motor driver in EV applications, as shown in [13]. Fig. 1 presents a block diagram showing the CSC combined with a hybrid converter for interfacing an EV and a RES. Regarding the EV charging, several controls can be considered aimed to preserve the batteries life cycle, such as the constant current and constant voltage (CC/CV) due to its simplicity and easy implementation [14]–[16]. On the other hand, regarding the RES interface, also several control algorithms can be considered, such as the maximum power point tracking (MPPT) based on the perturb and observe strategy [17][18].

This paper presents a single-phase CSC combined with a hybrid converter for interfacing an EV and a RES. Based on the power electronics structure, the interface with the power grid is only performed through the CSC, and in terms of operation modes, it is possible: (i) operation as SAPF; (ii) operation as EV charger (the EV is charged with power from the power grid); (iii) operation as EV discharger, where part of the stored power in the EV is injected into the power grid; (iv) operation as RES interface, injecting power into the power grid; (v) combined operation of the previous modes (for instance, charging the EV and operating as a SAPF at the same time).

In section 2 is described in detail the topology and in section 3 is presented the control algorithm for the single-phase CSC and the hybrid converter, as well as the compensation control theory. In section 4 are presented simulations results of the single-phase CSC. Finally, section 5 exposes the main conclusions.

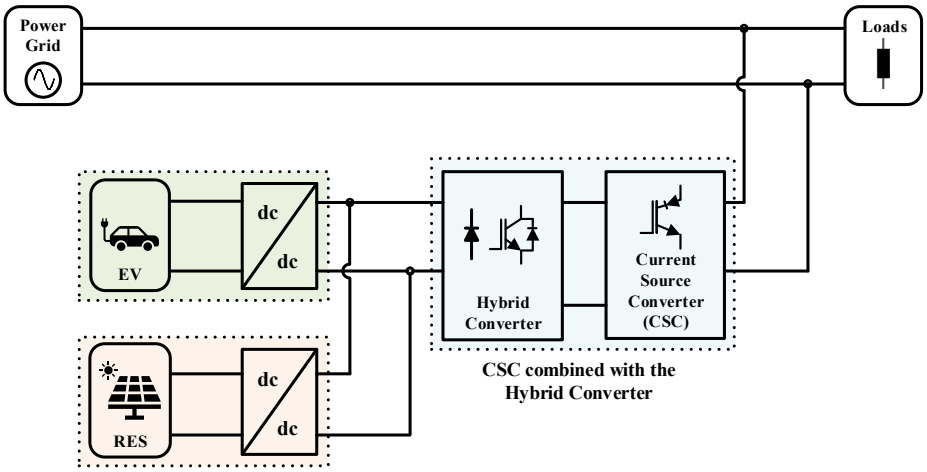


**Fig. 1.** Block diagram of the CSC combined with the hybrid converter on the dc-link, for interfacing an electric vehicle (EV) and a renewable energy source (RES) with the power grid.

## 2 Principle of Operation

In this section is described the topology presented in Fig. 2. As it can be seen, the topology consists of a CSC and a hybrid converter. The ac-dc converter is required for interfacing the power grid with the dc-link to compensate the current harmonics in the power grid and obtain a unitary power factor. This converter is composed by power semiconductors totally controlled, that it can be MOSFETs, IGBTs or RB-IGBTs. As this converter is unidirectional, when used IGBTs, it is crucial to guarantee block reverse, avoiding that the current flows by the antiparallel of IGBTs. For that reason, the use of RB-IGBTs is a viable solution allowing the reduction of costs, instead of using IGBTs in series with diodes [19][20]. On the other hand, the hybrid converter is bidirectional and it is composed by two diodes and two IGBTs. The aim of this converter is interfacing the EV, allowing the power absorption or injection in the power grid (discharging or charging of the EV) and interfacing the RES (extracting the maximum power) controlling the dc current in dc-link of the CSC. Thus, the hybrid converter has two modes of operation: (i) grid-to-vehicle (G2V) and (ii) vehicle-to-grid (V2G). During the G2V mode, the power is transferred from the power grid to the dc-link of the hybrid converter, where the dc-dc converter for the EV is connected. In this mode of operation is applied the CC/CV method, whose output of the control is a voltage reference for the dc-link of the hybrid converter. During the V2G mode, the power is transferred from the batteries to the power grid. For this operation mode, the output of the control is also a voltage reference applied to the dc-link of the hybrid converter. For both modes of operation, if the dc-link voltage ($v_{ev}$) is higher than the voltage reference, the IGBTs $S_5$ and $S_6$ are on, whereas if $v_{ev}$ is lower than the voltage reference both IGBTs are off. When $v_{ev}$ is equal to the voltage reference, it is only enabled one of the IGBTs, $S_5$ or $S_6$.

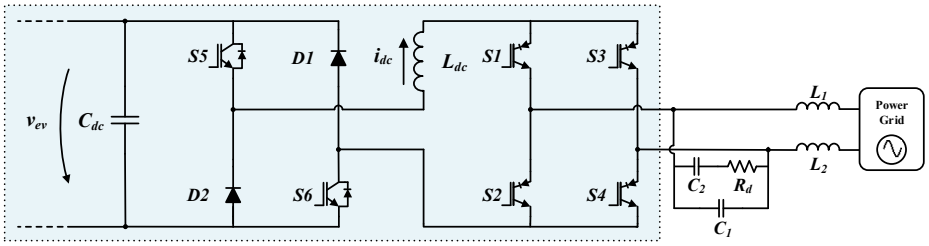


**Fig. 2.** Electrical schematic of the single-phase CSC combined with the hybrid converter.

## 3 Proposed Control Algorithm

This section introduces a detailed description of the control algorithm for the single-phase CSC interfacing the EV and RES, which is presented in Fig. 3. The control algorithm includes the control theory for the SAPF operation performed by the CSC, the charging of the EV using the CC/CV method and the extraction of the maximum point of the power from the RES through the MPPT control algorithm. The management of the power from/for the EV and the RES is made by the hybrid converter.

The operation of the SAPF is realized before and during the charging and discharging of the EV and the extraction of the power from the RES. For the correct operation of the SAPF, it is required a method of synchronization with the power grid. In this case, it is used the E-PLL algorithm [21]–[23] whose input signal is the power grid voltage ($v_s$). The dc-link regulation ($p_{reg}$) is obtained with a PI controller, where the input signals are the dc-link current ($i_{dc}$) and its reference ($i_{dc}^*$). Based on the E-PLL ($v_{pll}$) and the load current ($i_L$), it is calculated the compensation current ($i_c$) through the theory of Fryze-Buchholz-Depenbrock (FBD) approached in [24]–[26]. The commutation of the power semiconductors of the CSC is obtained from the modulation block of the SAPF. The hybrid converter is controlled for the EV charging following the two stages of the CC/CV method and for the EV discharging. As it can be observed, the variables needed to control the hybrid converter are the EV current ($i_{ev}$), the EV reference current ($i_{ev}^*$) and the EV voltage ($v_{ev}$). Moreover, it is measured the voltage ($v_{RES}$) and the current ($i_{RES}$) on RES for the calculation of the power provided by the RES and thus, compare the power obtained with the power calculated in the previous time in order to extract the maximum power and inject power in the power grid. In the following items are described with more detail the power theories used for both converters.

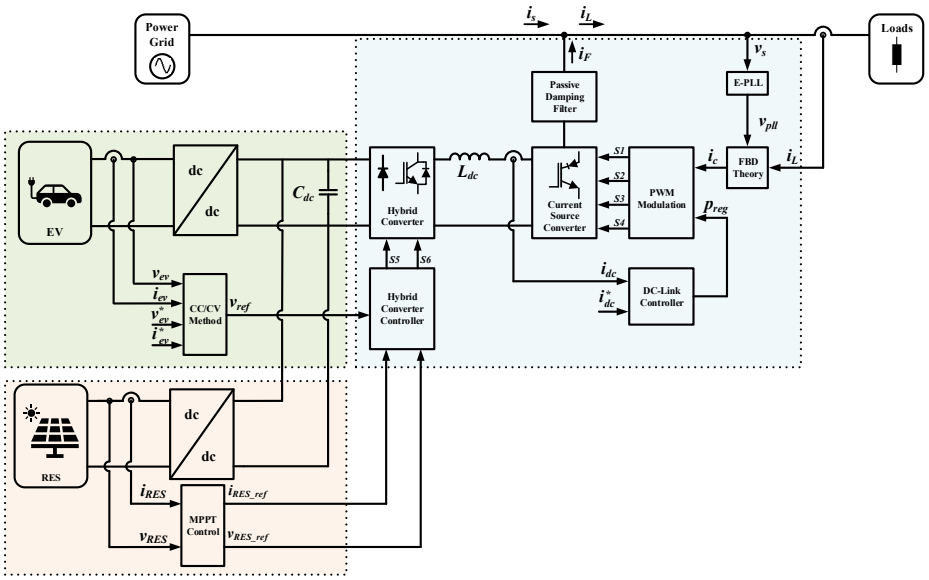


**Fig.**

### 3.1 Control when the CSC is Operating as Shunt Active Power Filter

The SAPF is responsible for supplying the harmonics and reactive power required by the loads. For that, the SAPF must be capable of producing the compensation current in order to obtain a power grid current sinusoidal and in phase with the power grid voltage. The compensation current is calculated through a power theory, that in this case is the Fryze theory. The principle of this theory is that a load can be represented by an equivalent conductance ($G_a$) in parallel with a current-source. In order to apply this power theory, it is calculated the active power multiplying the output of the E-PLL ($v_{pll}$) by the load current ($i_L$), calculating subsequently, the average active power ($P$) through the sliding window method. The $G_a$ is obtained through the $P$ and the squared RMS value of the power grid voltage ($v_s^2$), as it can be seen in $Ga = \frac{P}{v_s^2}$. (1).

$$G_a = \frac{P}{v_s^2}. \tag{1}$$

The active current ($i_a$) associated to the $G_a$ is presented in $ia = G_a\, v_s$. (2).

$$i_a = G_a\, v_s. \tag{2}$$

Finally, the compensation current ($i_c$) produced by the SAPF is determined by $ic = i_L - i_a$. (3) which corresponds to the difference between the load current ($i_L$) and active current ($i_a$).

$$i_c = i_L - i_a. \tag{3}$$

### 3.2 Control when the Hybrid Converter is Operating as EV Charger or Discharger

The hybrid converter is bidirectional and allows the charging and discharging of the EV with controlled current. The dc-dc converter of the EV is connected in parallel with the dc-link of the CSC. Due to the advantages of the CC/CV method such as its simplicity, easy implementation and the fact that it is adequate for the majority of batteries used in EV, this method was studied and applied in this work. Initially, it is applied a constant current for the EV and the EV voltage increases since reach the maximum charging voltage for the used batteries. After that, the constant current mode is replaced by the constant voltage mode, where the EV current starts decreasing exponentially, maintaining the EV voltage. The EV charging process finishes when the EV current reaches the residual batteries current. During the CC mode, the error is obtained by the subtraction between the reference current ($i_{ev}^{*}$) and the EV current ($i_{ev}$). Subsequently, the error is used by the PI controller, where it is adjusted the gains, *kp* and *ki*, allowing that the EV current follows the established reference ($i_{ev}^{*}$). The output of the PI controller is the reference voltage ($v_{ev}^{*}$) which is compared with EV voltage, whose comparison determines the states of the power semiconductors that composes the hybrid converter. In $if\, v_{ev} < v_{ev}^{*},\ S_5 = 0 \wedge S_6 = 0 \ if\ v_{ev} > v_{ev}^{*},\ S_5 = 1 \wedge S_6 = 1 \ if\ v_{ev} = v_{ev}^{*},\ S_5 = 0 \wedge S_6 = 1$. (4) is showed the conditionals for the commutations of the aforementioned semiconductors. When reached the maximum EV voltage, it is initialized the CV mode whose control is also carried out by the PI controller. In this case, the control variable is the EV voltage instead of the EV current, as previously described for the CC mode.

$$\begin{cases} if\ v_{ev} < v_{ev}^{*},\ S_5 = 0 \wedge S_6 = 0 \\ if\ v_{ev} > v_{ev}^{*},\ S_5 = 1 \wedge S_6 = 1. \\ if\ v_{ev} = v_{ev}^{*},\ S_5 = 0 \wedge S_6 = 1 \end{cases} \quad (4)$$

### 3.3 Control when the Hybrid Converter is Operating as RES Interface

Another application of the hybrid converter is the interface of the RES in order to extract the maximum power and to inject in the power grid or charging the EV. For that, it is necessary to implement a control algorithm designated MPPT. The MPPT algorithm aims to identify constantly the maximum power point of the RES and allows that the hybrid converter operates correctly. There are several MPPT control algorithms which are approached in [17][27][28]. The main differences presented in these MPPT algorithms are the costs, efficiency as well as the complexity of implementation.

## 4 Simulation Results

In this section are presented the main simulation results of the topology simulated with the PSIM software. The presented simulations were performed for the main conditions of operation of the CSC and the hybrid converter, specifically considering the

EV charging and discharging processes and including the compensation of the current harmonics and power factor in the power grid. Table **1** shows the specifications of the developed simulation model.

Initially, the hybrid converter had as main contribution to reduce the inductance value of the inductor in dc-link of the CSC. However, the following results prove that the same converter apart from allowing the reduction of the inductor in dc-link, the hybrid converter is also advantageous for interface other dc systems, like the interface of an EV interface and the interface of a RES. In order to validate the CSC operating as SAPF and the EV charging process, the presented simulation results in this paper consist of: (i) Dc-link current regulation; (ii) Compensation of harmonic currents and low power factor in the power grid by the CSC operating as SAPF; (iii) EV charging and discharging along with the harmonic compensation by the CSC operating as SAPF.

As nonlinear load connected to the power grid, it was considered a full-bridge rectifier with a RC load (168 Ω, 2.6 mF), with a coupling inductor of 0.5 mH, as well as a RL load in parallel (12.5 Ω, 70 mH). Table 2 shows the specifications of the dc-link of both converters, including the values of components that composes the passing damping filter. This coupling filter was introduced in order to reduce the losses and the electromagnetic interference caused by the CSC as approached in [29].

**Table 1.** Specifications of the CSC interfacing EV and RES.

| **Parameters** | **Value** | **Unit** |
|---|---|---|
| RMS Grid Voltage | 230 ± 10% | V |
| Grid Frequency | 50 ± 1% | Hz |
| Output dc Voltage Range | 0 to 450 | V |
| Switching Frequency | 40 | kHz |

**Table 2.** Specifications of the power converters.

| Parameters | **Value** | **Unit** |
|---|---|---|
| Inductor $L_{dc}$ | 100 | mH |
| Capacitor $C_{dc}$ | 300 | µF |
| Damping Resistor $R_d$ | 15 | Ω |
| Inductors $L_1$, $L_2$ | 20 | µH |
| Capacitor $C_1$ | 5 | µF |
| Capacitor $C_2$ | 20 | µF |

One of the roles of the CSC is to control and maintain the current in the dc-link at an acceptable value. The current in dc-link ($i_{dc}$) is presented in Fig. **4**, which is regulated through the PI controller. As it can be observed, when starts the EV charging, i.e., during the transient-state, the dc-link current decreases, however the dc-link current quickly reaches the reference current of 50 A.

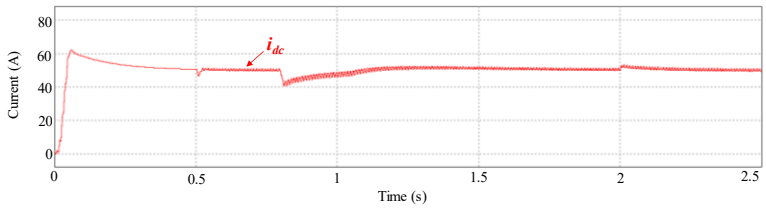


**Fig. 4.** Simulation results of the dc-link current ($i_{dc}$).

In Fig. **5** are presented the simulation results of the power grid voltage ($v_g$) and grid current ($i_g$) before compensation. As it can be observed, the power grid current is not sinusoidal and in phase with the power grid voltage. The power grid current presents a $THD_{\%f}$ of 36%. The RMS value of the $i_g$ is 10.4 A. As mentioned above, having a high harmonic distortion in the power grid can result in increasing losses, and in possible damage of equipment connected to the installation.

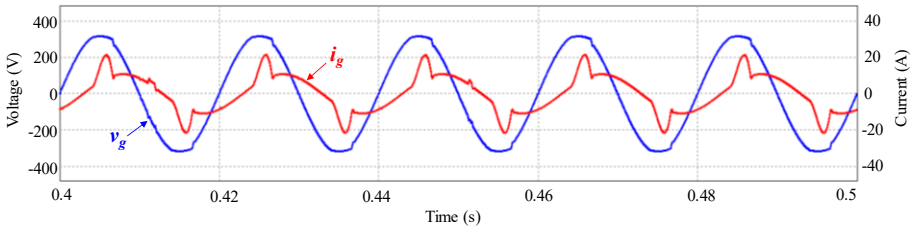


**Fig. 5.** Simulation results of the power grid voltage ($v_g$) and grid current ($i_g$) before compensation, and without the EV charging process and injection of power from RES.

After the dc-link regulation, the SAPF produces a compensation current in order to compensate the current harmonics in the power grid. Fig. **6** shows $v_g$ and $i_g$ after compensation, where the power grid current is almost sinusoidal and in phase with the power grid voltage. The RMS value of the $i_g$ is 7.35 A. The $THD_{\%f}$ in the power grid current is reduced from 36% to 5.69%, corresponding to an important improvement.

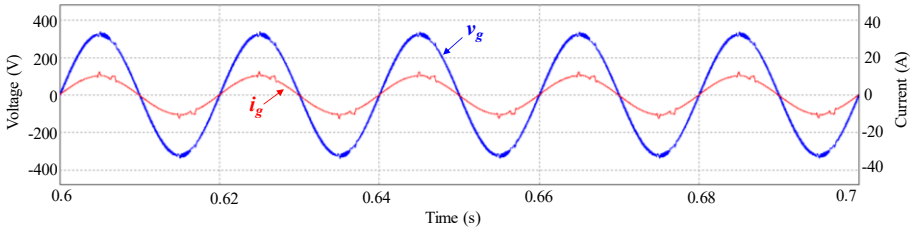


**Fig. 6.** Simulation results of the power grid voltage ($v_{ga}$) and grid current ($i_{ga}$) after compensation, and without the EV charging process and injection of power from RES.

Fig. 7 shows the G2V (1 and 2) and V2G (3) modes, where $i_{ev}$ is the EV current and $v_{ev}$ is the EV voltage. During G2V operation mode (from 0.8 s to 2 s), the EV are

charged for a reference current of 10 A with a minimum voltage of 250 V. The EV charging process consists of two charging stages, namely constant current (1) followed by constant voltage (2). Initially, the EV is charged with a current of 10 A, whose power is supplied by the power grid and the RES. When the voltage in the EV reaches the maximum voltage of 450 V, the EV current starts decreasing until reaches approximately 0 A (constant voltage). This method is very advantageous for the charging of lithium batteries, that are very common in EV. During V2G mode (from 2 to 2.5 s), the power from the EV is injected into the power grid for a reference current of 2 A, which corresponds to the stage (3). As it can be observed during the discharging of the EV, the $v_{ev}$ decreases. During all modes (1, 2 and 3), the CSC is controlled to operates as SAPF, i.e., compensates the current harmonics in the power grid and to obtain an unitary power factor.

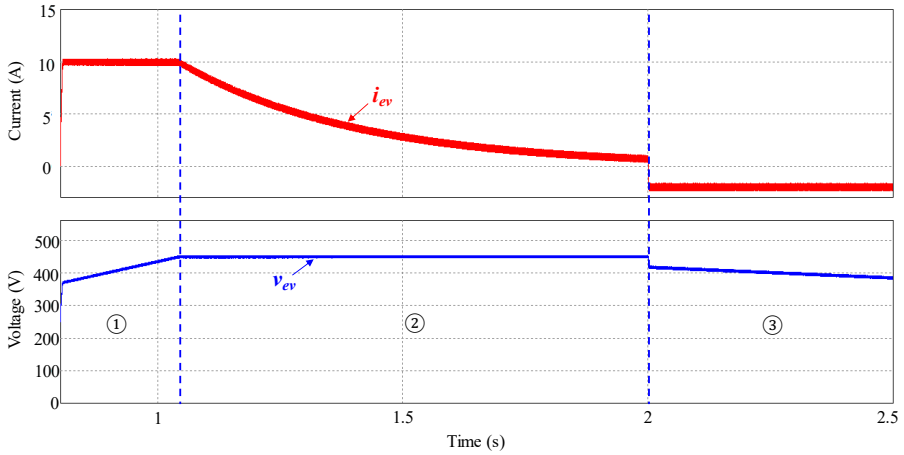


**Fig. 7.** Simulation results of a Lithium battery charging and discharging process: (1) CC stage; (2) CV stage and (3) EV discharging.

During the EV charging and injection of power in the power grid, it cannot be neglected the power quality improvement. So, the SAPF continuing operating and the harmonic current in power grid is compensated. In Fig. 8 are showed $v_g$ and $i_g$ after compensation during EV charging process. The power grid current presents a low $THD_{\%f}$ of 2.48%, which is very significantly reduced, as it is intended. On the other hand, the RMS value of the $i_g$ increased to 26.7 A.

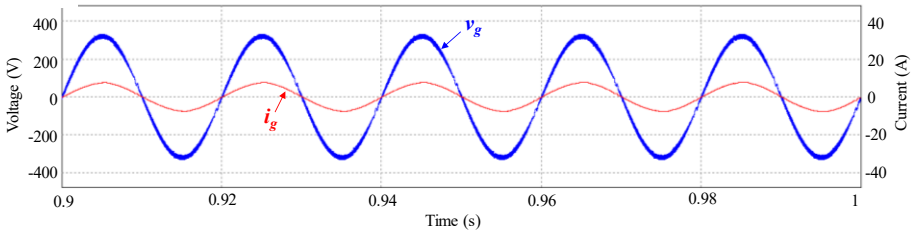


**Fig. 8.** Simulation results of the power grid voltage ($v_g$) and grid current ($i_g$) after compensation, and during the EV charging process without injection of power from RES.

Finally, it is carried out the injection of power from the EV and RES, where it is also effectuated the compensation of the harmonic currents in the power grid side. Fig. 9 presents the $v_g$ and $i_g$ after compensation, where $i_g$ is in phase with $v_g$, whose $THD_{\%f}$ value is of 7.91%. As it intended, the RMS value of the $i_g$ is reduced to 4 A.

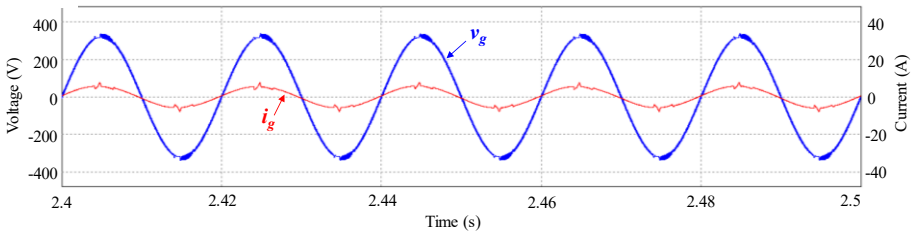


**Fig. 9.** Simulation results of the power grid voltage ($v_g$) and grid current ($i_g$) after compensation, and during the injection of power in the power grid from EV and RES.

## 5 Conclusions

This paper presents a single-phase current-source converter (CSC) with a hybrid converter on the dc-link to interface an electric vehicle (EV) and a renewable energy source (RES). The CSC can be controlled as shunt active power filter for compensating current harmonics and low power factor, and also to allow the bidirectional operation for the EV and RES interface. On the other hand, the hybrid converter permits the interface of the dc-link of the CSC with the dc-dc converters for the interface of the EV and RES. Taking into consideration the preservation of the batteries lifetime, the constant current and constant voltage (CC/CV) control was adopted. Regarding the RES interface, it was implemented a maximum power point tracking circuit. The topology and the operation principles are described along the paper, and simulation results are presented. The obtained results show the correct operation of the CSC operating as shunt active power filter, as well as operating in bidirectional mode to interface the EV and the RES.

## References


[1] Afonso, João L. Sustainable Energy for Smart Cities: First EAI International Conference, *SESC 2019, Braga, Portugal, December 4–6, 2019, Proceedings. Springer Nature, 2020*.

[2] Monteiro, V., Pinto, J. G., Exposto, B., Gonçalves, H., Ferreira, J. C., Couto, C., & Afonso, J. L. (2012, October). Assessment of a battery charger for electric vehicles with reactive power control. *In IECON 2012-38th Annual Conference on IEEE Industrial Electronics Society* (pp. 5142-5147). IEEE.

[3] Strasser, T., Andrén, F., Kathan, J., Cecati, C., Buccella, C., Siano, P., Mařík, V. (2014). A review of architectures and concepts for intelligence in future electric energy systems. *IEEE Transactions on Industrial Electronics, 62*(4), 2424-2438.

[4] V. Monteiro, J. G. Pinto, B. Exposto, and J. L. Afonso, "Comprehensive comparison of a current-source and a voltage-source converter for three-phase EV fast battery chargers," *Proc. - 2015 9th Int. Conf. Compat. Power Electron. CPE 2015*, no. June, pp. 173–178, 2015.

[5] P. S. Moses, S. Deilami, A. S. Masoum, and M. A. S. Masoum, "Power quality of smart grids with plug-in electric vehicles considering battery charging profile," *IEEE PES Innov. Smart Grid Technol. Conf. Eur. ISGT Eur.*, pp. 1–7, 2010.

[6] V. Monteiro, J. G. Pinto, B. Exposto, L. F. C. Monteiro, C. Couto, and J. L. Afonso, "A Novel Architecture of a Bidirectional Bridgeless Interleaved Converter for EV Battery Chargers," *IEEE Int. Symp. Ind. Electron.*, vol. 2015-Septe, pp. 190–195, 2015.

[7] B. Exposto, V. Monteiro, J. G. Pinto, D. Pedrosa, A. A. N. Meléndez, and J. L. Afonso, "Three-phase current-source shunt active power filter with solar photovoltaic grid interface," *Proc. IEEE Int. Conf. Ind. Technol.*, vol. 2015-June, no. June, pp. 1211–1215, 2015.

[8] B. Exposto, J. G. Pinto, V. Monteiro, D. Pedrosa, H. Gonçalves, and J. L. Afonso, "Experimental and Simulation Results of a Current-Source Three-Phase Shunt Active Power Filter using Periodic-Sampling," *Annu. Semin. Autom. Ind. Electron. Instrum. 2012 - SAAEI'12, pp. 380-385, Guimarães, Port.*, pp. 380–385, 2012.

[9] B. Exposto, J. G. Pinto, D. Pedrosa, V. Monteiro, H. Goncalves, and J. L. Afonso, "Current-source shunt active power filter with periodic-sampling modulation technique," *IECON Proc. (Industrial Electron. Conf.*, pp. 1274–1279, 2012.

[10] S. Pettersson, M. Salo, and H. Tuusa, "Optimal DC current control for four-wire current source active power filter," *Conf. Proc. - IEEE Appl. Power Electron. Conf. Expo. - APEC*, pp. 1163–1168, 2008.

[11] C. F. Oliveira, L. A. M. Barros, J. L. Afonso, J. G. Pinto, B. Exposto, and V. Monteiro, "A Novel Single-Phase Shunt Active Power Filter Based on a Current-Source Converter with Reduced Dc-Link," *Lect. Notes Inst. Comput. Sci. Soc. Telecommun. Eng. LNICST*, vol. 315 LNICST, pp. 269–280, 2020.

[12] G. J. Su and L. Tang, "Current source inverter based traction drive for EV battery charging applications," *2011 IEEE Veh. Power Propuls. Conf. VPPC 2011*, pp. 1–6, 2011.

[13] L. Tang and G. J. Su, "Boost mode test of a current-source-inverter-fed permanent

magnet synchronous motor drive for automotive applications," *2010 IEEE 12th Work. Control Model. Power Electron. COMPEL 2010*, 2010.

[14] W. Shen, T. T. Vo, and A. Kapoor, "Charging algorithms of lithium-ion batteries: An overview," *Proc. 2012 7th IEEE Conf. Ind. Electron. Appl. ICIEA 2012*, pp. 1567–1572, 2012.

[15] J. G. Pinto *et al.*, "Bidirectional battery charger with Grid-to-Vehicle, Vehicle-to-Grid and Vehicle-to-Home technologies," *IECON Proc. (Industrial Electron. Conf.*, pp. 5934–5939, 2013.

[16] J. S. Moon, J. H. Lee, I. Y. Ha, T. K. Lee, and C. Y. Won, "An efficient battery charging algorithm based on state-of-charge estimation for electric vehicle," *2011 Int. Conf. Electr. Mach. Syst. ICEMS 2011*, 2011.

[17] A. K. Abdelsalam, A. M. Massoud, S. Ahmed, and P. N. Enjeti, "High-performance adaptive perturb and observe MPPT technique for photovoltaic based microgrids," *IEEE Trans. Power Electron*., vol. 26, no. 4, pp. 1010–1021, Apr. 2011.

[18] T. Esram and P. L. Chapman, "Comparison of Photovoltaic Array Maximum Power Point Tracking Techniques," *IEEE Trans. Energy Convers.*, vol. 22, no. 2, pp. 439–449, Jun. 2007.

[19] M. Routimo, M. Salo, and H. Tuusa, "Comparison of voltage-source and current-source shunt active power filters," *IEEE Trans. Power Electron.*, vol. 22, no. 2, pp. 636–643, 2007.

[20] M. Salo and S. Pettersson, "Current-source active power filter with an optimal DC current control," *PESC Rec. - IEEE Annu. Power Electron. Spec. Conf.*, 2006.

[21] H. Carneiro, L. F. C. Monteiro, and J. L. Afonso, "Comparisons between synchronizing circuits to control algorithms for single-phase active converters," *IECON Proc. (Industrial Electron. Conf.*, pp. 3229–3234, 2009.

[22] M. Karimi-Ghartemani, S. A. Khajehoddin, P. K. Jain, A. Bakhshai, and M. Mojiri, "Addressing DC component in pll and notch filter algorithms," *IEEE Trans. Power Electron.*, vol. 27, no. 1, pp. 78–86, 2012.

[23] M. Karimi-Ghartemani and M. R. Iravani, "A method for synchronization of power electronic converters in polluted and variable-frequency environments," *IEEE Trans. Power Syst.*, vol. 19, no. 3, pp. 1263–1270, 2004.

[24] L. S. Czarnecki, "Budeanu and Fryze : Two frameworks for interpreting power properties of circuits with nonsinusoidal voltages and currents," *Electr. Eng.*, vol. 80, no. Teoria de Potência;, pp. 359–367, 1997.

[25] J. Zhou, Z. Wang, and X. Fu, "Study on the improved harmonic detection algorithm based on FBD theory," *Asia-Pacific Power Energy Eng. Conf. APPEEC*, no. 1, pp. 2–5, 2011.

[26] V. Staudt, "Fryze - Buchholz - Depenbrock : A time-domain power theory," pp. 1–12, 2008.

[27] D. Sera, R. Teodorescu, J. Hantschel, and M. Knoll, "Optimized maximum power point tracker for fast-changing environmental conditions," *IEEE Trans. Ind. Electron*., vol. 55, no. 7, pp. 2629–2637, Jul. 2008.

[28] S. Li, B. Zhang, T. Xu, and J. Yang, "A new MPPT control method of photovoltaic grid-connected inverter system," in *The 26th Chinese Control and Decision Conference (2014 CCDC)*, 2014, pp. 2753–2757.

[29] N. Hensgens, M. Silva, J. A. Oliver, J. A. Cobos, S. Skibin, and A. Ecklebe, “Optimal design of AC EMI filters with damping networks and effect on the system power factor,” *2012 IEEE Energy Convers. Congr. Expo. ECCE 2012*, vol. 7, no. 2, pp. 637–644, 2012.